**Fluorescence-Based Detection of Fusion State on a Cryo-EM Grid using Correlated Cryo-Fluorescence and Cryo-Electron Microscopy**

Lauren Ann Metskas and John A. G. Briggs

**Supplemental Information**

1. DiD Fluorophore Characterization

2. Fusion Assay for Virus-Like Particles and 5% DiD Vesicles

3. Materials and Methods:
    -Fluorophore Stock Preparation
    -Vesicle Preparation
    -Buffer Titration Curve for pH Control
    -Virus-Like Particle Preparation
    -Fluorophore Assessments
    -Fusion Assays
    -Cryo-EM/cryo-CLEM Grid Preparation
    -Cryo-Fluorescence Microscopy and Intensity Analysis
    -Cryo-Electron Microscopy and Correlation with cryo-FM

## 1. DID FLUOROPHORE CHARACTERIZATION

To assess the quenching behavior of DiD, labeled 1 mg/mL POPC vesicle preparations with varying molar percentages of DiD: 0.5, 1, 2, 3, 5, 7.5, 10, and 12.5 mol%, and used buffers at pH from 5.1-7.5 (the pH range relevant for endosomal escape; see SI). Vesicle preparations were mixed 1:1 with citrate-HEPES buffer and measured in a Synergy HT plate reader to monitor total brightness relative to fluorophore content (BioTek, monochromator excitation 644 nm, emission 670 nm, background correction 500 nm, average of 10 reads).

The total fluorescence of the vesicle samples rose from 0.5% to 3% DiD, then dropped to a lower intensity plateau for concentrations 5% -12.5% with little fluorescence gain from fluorophore added past 5% (Figure S1A). Importantly, the total fluorescence in the cuvette was lower for the higher-DiD concentrations, where the sample is quenched, than for the dequenched samples, even when the total amount of fluorophore was an order of magnitude larger. We conclude that if the molar percentage of DiD is above roughly 5%, then variation in total fluorophore amount due to heterogeneity in vesicle or virion sizes will be small in comparison with the large intensity shifts that would occur if the dye dequenches due to dilution upon fusion with a target membrane (Figure S1). However, intensities in post-fusion states could vary more widely based on the initial fluorophore amount.

When measurements were normalized according to total fluorophore concentration (as determined by absorbance at 645 nm), a linear decrease in fluorophore brightness from 0.5% to 5% was visible, with a dark plateau at concentrations 5% and above, and a total intensity difference of roughly 10-fold between 5% and 0.5% DiD (Figure S1B). The effect of pH was minimal compared to that of concentration (Figure S1). In the context of a fusion sample, fusion between a 5% DiD vesicle and a virion of similar size, both smaller than the point-spread function of the cryo-FM, would result in a roughly 10-fold increase in fluorescence at that location (Figure S1B). Other size relationships would be dependent upon both the dilution factor of the DiD upon fusion according to target surface area, and distribution of fluorescence intensity over the imaging area of the fused membranes.

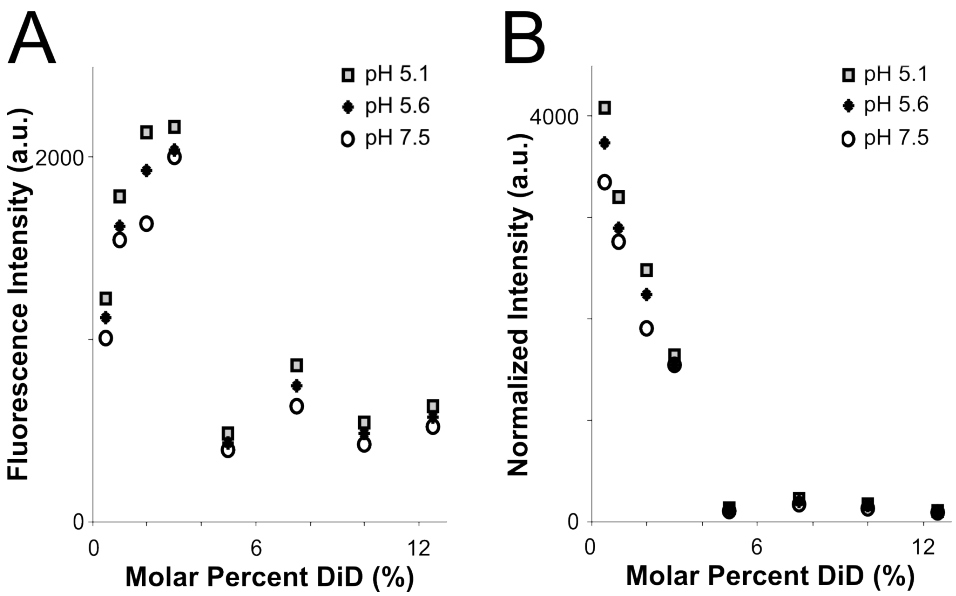


***Figure S1*. Fluorophore quenching at room temperature. A:** Fluorescence intensity of vesicles with varying lipid concentration. Even as the total fluorophore concentration of the sample increases, autoquenching at 5% DiD results in lower total fluorescence intensity. **B:** Results from **A**, normalized to equal fluorophore concentration (varying total lipid concentration). Autoquenching is linear from 0.5-5% DiD, at which point the dye is fully quenched.

## 2. FUSION ASSAY FOR VIRUS-LIKE PARTICLES AND 5% DID VESICLES

Fusion assays were performed to confirm VLP function and DiD dequenching signal at room temperature under fusion conditions. Briefly, 80 µL fusion mix was prepared using 50 µM target membrane lipid (2.5 µM DiD, see methods above), pH 7.5 HEPES-citrate buffer, and a volume of VLPs corresponding to 0.014 mg accessible protein. The mix was prepared in the wells of a 96-well plate, which was then loaded immediately into a plate reader (BioTek, Synergy H1). After a five-minute incubation at 37 C, the mix was acidified to pH 5.1 by injection of 45 µL of pH 3 HEPES-citrate buffer. The plate was shaken for 15 s to mix, followed by reads every 30 s for 20 minutes (620/40 excitation, 680/30 emission, gain 35). Finally, the plate was removed and 0.5% Triton X-100 was added to the wells with pipetting to lyse the vesicles and VLPs.

Assays were normalized for total fluorophore concentration by subtracting the pre-acidification intensity and dividing by the intensity following lysis with 0.5% Triton X-100, which corresponds to complete dequenching. The acidification results in hemifusion between VLPs and liposomes, dequenching the dye as it is distributed into a larger lipid pool (progression of hemifusion to fusion is typically assumed but not directly monitored by dequenching of a single intercalated dye). The VLPs displayed robust and rapid achievement of hemifusion, reaching a fluorescence intensity plateau by 3 minutes post-acidification (Figure S2).

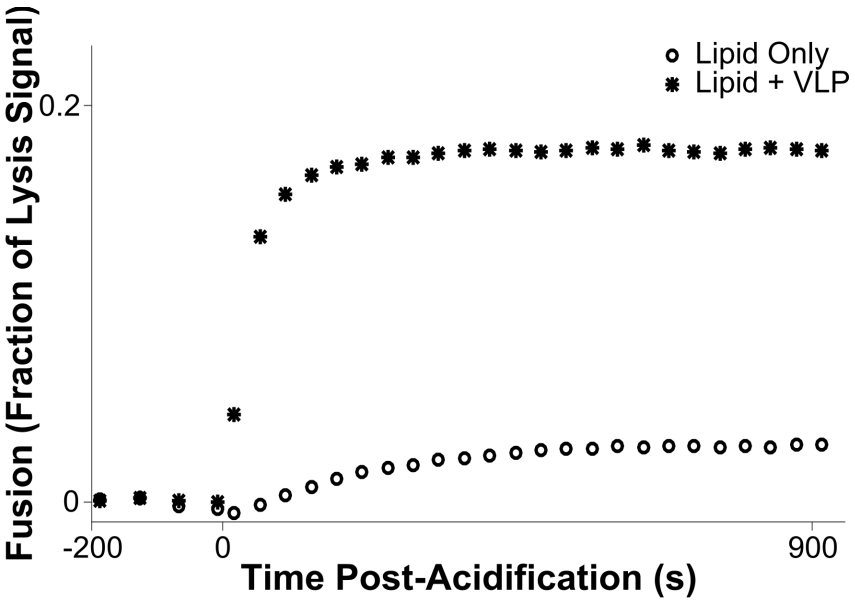


***Figure S2*. Kinetic assay for hemifusion between influenza VLPs and 5% DiD liposomes**. Fusion is stimulated by acidification to pH 5.1 at time = 0 s.

## 3. MATERIALS AND METHODS

### Fluorophore Stock Preparation

*R18*
Octadecyl Rhodamine B Chloride (R18, Thermo Fisher Scientific) was solubilized in 100% ethanol at roughly 10 mg/mL and stored at -80 C in glass vials sealed with Teflon tape for up to 1 month. Exact concentration was determined by measuring absorbance in methanol, using the manufacturer's extinction coefficient under these conditions.

*DiD*
DiIC18(5) solid (1,1'-Dioctadecyl-3,3,3',3'-Tetramethylindodicarbocyanine, 4-Chlorobenzenesulfonate Salt, Thermo Fisher Scientific) was solubilized in 100% ethanol at roughly 5 mM and stored at -20 C in glass vials sealed with Teflon tape. Exact concentration was determined by measuring absorbance in methanol (1 µL stock in 1.5 mL methanol), using the manufacturer's extinction coefficient under these conditions.

### Vesicle Preparation

*POPC vesicles (Figures 1, S1)*
1-palmitoyl-2-oleoyl-sn-glycero-3-phosphocholine (Avanti Lipids) was dissolved in chloroform at 1 mg/mL concentration, then dried into a thin film in a round-bottom flask by evaporation using nitrogen gas. This thin film rested overnight in a room-temperature dessicator. Following evaporation, the POPC film was incubated in TNE buffer (50 mM Tris-HCL pH 7.4, 100 mM NaCl, 0.1 mM EDTA) for 30 minutes at 4 C, then subjected to 7 cycles of freeze/thaw by alternating baths in an acetone/dry ice mixture and warm water. The resulting lipid mixture was extruded for 21 passes through a membrane with a pore size 50-200 nm depending upon the experiment (Avanti Lipids). Average vesicle size and quality were confirmed by dynamic light scattering (DLS, see below).

For Figure 1B, a mixture of 90% POPC / 10% POPS was used to decrease the clumping tendency of fully POPC vesicles, allowing better quantification of fluorescence intensity from separated vesicles on the EM grid.

For DiD-labeled vesicles, the desired amount of fluorophore was incorporated into the chloroform/methanol mixture immediately prior to drying. For R18-labeled vesicles, fluorophore was added to a glass autosampler vial with the extruded vesicle mixture and stirred for 30 minutes at room temperature. Following labeling, aggregates and any unincorporated fluorophore were removed by passing vesicles through two consecutive 0.5 mL 7K MWCO Pierce Zeba columns, following manufacturer's protocols.

*Lipid vesicles for hemifusion experiments (Figures 2, S2).*
The lipid composition for these vesicles was adapted from Chlanda et al. 2016 (1). A mixture of 47% POPC / 13% POPE / 35% cholesterol / 5% total ganglioside (Avanti Lipids) was prepared in a mixture of roughly 1 mg/mL in 2 parts chloroform / 1 part methanol; 5%

DiD was then added to this mixture prior to drying into a thin film overnight as above. Lipid vesicles were prepared by extrusion as above, using a buffer of 10 mM HEPES / 50 mM sodium citrate / 150 mM NaCl at pH 7.5 (2) and a 100 nm pore size. Vesicle preparations were filtered by spin column as above.

Vesicle concentration was estimated by DiD absorbance at 645 nm, assuming the 5% molar composition.

*Vesicle Size Assessment*
We prepared a comparison of vesicle sizes by DLS on a Zetasizer (Malvern Panalytical). Briefly, 100 µL of an unlabeled vesicle preparation (nominally 1 mg/mL) were measured for 3 sets of 13 reads. By this method, a 100 nm membrane produced vesicles with a mean diameter of 163.4 nm, with polydispersity of 0.144 (roughly 62 nm standard deviation).

We then imaged this vesicle preparation on a cryo-EM grid. A mixture of 1.5 µL vesicle preparation and 1.5 µL 10 nm gold fiducial marker was pipetted onto a C-Flat 2/2-300C EM grid, blotted in a Vitrobot (Mark 2, offset -4, 3 s blot time, >85% humidity, 15 C), and plunged into liquid ethane. The resulting grid was imaged on a FEI Tecnai T12 microscope at 12.5 A pixel size (9800x magnification), and vesicle sizes were measured using Amira software. We found that the vesicles on the grid had a mean diameter of $88 \pm 36$ nm.

We believe that this strong contrast in vesicle sizes is due to systematic biases in both instruments. Briefly, DLS can over-estimate a vesicle diameter based on charge and hydration shells, and vesicle-vesicle association might also result in larger vesicle sizes without severely increased polydispersity if these interactions are transient. On the other hand, we expect that large lipid vesicles are selected against during cryo-EM imaging, possibly due to increased contact with the blotting paper, greater exposure to the air-water interface, or preferential localization to areas of thick ice.

**Buffer Titration for pH Control**

We elected to use a HEPES-citrate dual-buffer system (10 mM HEPES / 50 mM sodium citrate / 150 mM NaCl) to control pH over a greater range, as in (2). pH is adjusted by addition of acidic buffer to the neutral buffer containing the sample, thus avoiding osmotic stress. A titration curve was measured using a pH electrode, and was found to be linear within the pH range suitable for viral fusion experiments. For these experiments, buffers at pH 7.5 and pH 3 were used. The linear regression variables are an intercept of pH 6.4 (due to non-linearity outside the 10-50% range) and a slope of -0.036 pH units per percent acidic buffer (Figure S3).

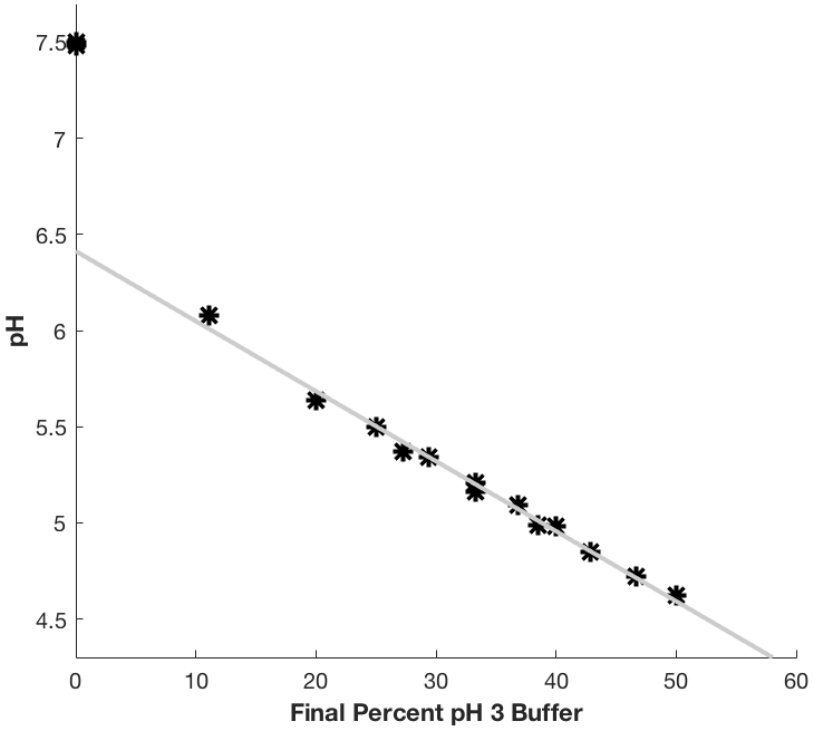


***Figure S3:*** **Titration curve for citrate/HEPES/NaCl buffer.** The pH of neutral buffer can be specifically and reproducibly adjusted by addition of pH 3 buffer on a volume:volume basis.

**Virus-Like Particle (VLP) Preparation**

VLPs were prepared by transfection of influenza A proteins into HEK cells by adapting a previously described protocol (3). PCAGGS plasmids for influenza A hemagglutinin (A/Hong Kong/1/68, HA), neuraminidase (A/Singapore/1/57, NA), and matrix proteins 1 (A/Hong Kong/1/68, M1) and 2 (A/Hong Kong/1/68, M2) were transfected into $1*10^6$ HEK 293T cells in serum-free DMEM, with 2.2 µg HA, 2.2 µg NA, 4.4 µg M1, and 1.1 µg M2 DNA per plate and using 30 µL FuGene according to manufacturer's instructions (Promega Corporation). Following transfection, a final concentration of 100 mU/µL exogenous NA (New England BioLabs, P0720S) was added to the plates to facilitate VLP release.

After 48 hours, the VLPs were treated with trypsin to cleave the HA subunits (1). Inhibited trypsin and cellular debris were removed by centrifugation at 900 xG for 10 minutes; VLPs were then harvested by centrifugation over a 32.5% sucrose cushion (SW40i rotor, 30k RPM, 90 minutes). VLP pellets were overlaid with citrate-HEPES buffer (above), allowed to rest overnight, and then resuspended gently with wide-mouthed pipet tips. VLP preparations were cleaned of excess sucrose and soluble proteins by a 4-hour dialysis against citrate-HEPES buffer using a 300 MWCO membrane, and gently concentrated in Microcon 100 MWCO concentrators (EMD Millipore) using a rotor speed of no more than 900 xG. VLPs prepared in this manner retained their mixed morphology (spheres and long filaments).

VLP concentrations were approximated by monitoring accessible surface protein concentration using a Bio-Rad Protein Assay according to manufacturer's instructions.

**Cryo-EM/cryo-CLEM Grid Preparation**

For the quenched lipid-only grid (Figure 1B), fluorescent signals were of roughly even intensity across the grid, making fiducial-free alignments difficult as vesicles appeared identical to each other by both EM and FM. We therefore used fluorescent fiducial markers to assist with high-precision correlation (4, 5). Briefly, a purchased stock solution of 50 nm Tetraspec beads was sonicated for 5 minutes in a waterbath sonicator, and Protochip C-Flat grids (2/2, 300 mesh) were glow-discharged for 30 s at ~30 mA. The tetraspec solution was diluted 1:50 in PBS, and 10 µL drops were incubated on the grids for 15 minutes. Grids were back-side blotted, rinsed with two washes of deionized water, and allowed to dry prior to use.

All cryo-EM/cryo-CLEM grids were frozen using the protocol from the *Vesicle Size Assessment* section above.

For hemifusion grids, vesicles and VLPs were prepared as above, mixed, and incubated on ice at relative concentrations of 0.16 mg/mL accessible viral protein and 0.12 mM target membrane lipid for roughly 30 minutes. This provided ample time for VLPs and vesicles to adhere. The tubes were then brought to room temperature and acidified to pH 5.1 for 60 s, followed by addition of 10 nm Protein A-coated gold fiducial markers (Cell Microscopy core, University Medical Center Utrecht). The sample was then pipetted onto grids and frozen as above. The total time between acidification and freezing was roughly 2.5 minutes, in keeping with the kinetics of the hemifusion plateau at room temperature.

**Cryo-Fluorescence Microscopy and Intensity Analysis**

Cryo-fluorescence microscopy was performed on Leica DM 1200 or DM6 FS cryo-CLEM microscopes running LAS X software and an OrcaFlash 4.0 V2 SCMOS camera (Hamamatsu Photonics). Excitation intensities were adjusted as needed to avoid heavy oversaturation of the camera or devitrification from extended high-intensity illumination. Typically, white transmitted light exposures were 80-100 ms, green channel imaging (480/40, 505, 527/30 nm excitation, dichroic, emission filters, Tetraspecs) used 30% intensity with aperture 4 and exposure time of 0.8-1 s, red channel imaging (560/40, 585, 630/76 nm excitation, dichroic, emission filters, R18) used 17% intensity for 25 ms, and far-red channel imaging (620/60, 660, 700/75 nm excitation, dichroic, emission filters, DiD) used 17% intensity with aperture 4 and exposure times of 14 ms (hemifusion, Figure 2) or 150 ms (quenched vesicles, Figure 1B). Grids were focus-mapped using built-in software functions, and imaged in Z-stacks of 10-12 slices and ~1 µm step sizes.

Images of grid squares of interest were build using FIJI's built-in Max Intensity projection algorithm (6, 7). Full-grid maps for correlating on-the-fly were generated with the Fiji Stack Focuser plug-in.

Spot intensities were quantified in FIJI using the built-in 3D Surface Plot feature. Briefly, the maximum peak intensity was recorded for each location, searching within the area of accuracy predicted by the correlation software and informed by visible chromatic offsets in the cryo-CLEM. The local background was determined by the plateau nearest the peak in cases where multiple peaks were present; otherwise the local background was determined by averaging along the edge of the visualization box (extended to reach a plateau when necessary), using the same surface as the point of interest. Points of interest that were near to contamination (ice) or areas of bright fluorescence without lipid/protein density (from fluorescent crystalline ice or suspected reflections) were avoided. Reported peak intensities are of the background-subtracted maximum of the peak center.

**Cryo-Electron Microscopy and Correlation with Cryo-Fluorescence Microscopy**

Cryo-EM grids were imaged on an FEI Tecnai T12 microscope (hemifusion) or FEI Tecnai F20 microscope (quenched DiD vesicles) running SerialEM. Grids were mapped in full at 150X magnification, which was correlated with the white transmitted light cryo-FM map using SerialEM map registration functions (5).

From this point, workflows followed different paths depending upon the goal of the experiment. For quenched lipid grids where each vesicle's intensity needed to be quantified, it was necessary to image at a magnification where each individual vesicle would be visible irrespective of fluorescence. Therefore, grid squares of interest were imaged by a 5x5 montage at 6000X magnification on the F20 microscope, and all alignment with cryo-fluorescence images was performed during post-processing using Matlab cryo-CLEM correlation scripts (4).

For hemifusion grids, we sought to both prepare maps for later correlation and to image bright and dim spots at higher magnification. Grid squares of interest were mapped at 1200X and aligned on-the-fly at the T12 microscope using SerialEM registration points based on visible grid square features and defects. This rapid, fiducial-free approach provided an estimated 0.2-0.3 µm precision for the correlation, which was sufficient for the hemifusion sample. (While higher magnification and alignment with fiducials would provide more precise correlation, this is time-consuming and was found to be unnecessary for this sample.) The fluorescence map location was used to direct the stage to the expected position, at which point a 5000 X image was used to center the object closest to the expected position. The image was then collected with 30,000 X magnification (0.37 nm pixel size, ~10 e/$A^2$, -5 µm defocus). Matlab cryo-CLEM scripts were again used in post-processing to correlate all remaining points and confirm that the higher-magnification images truly corresponded to the fluorescence they were targeting. Final correlation accuracy varied by square and ranged from roughly 60-200 nm.

**Supplementary References**


1. Chlanda, P., E. Mekhedov, H. Waters, C.L. Schwartz, E.R. Fischer, R.J. Ryham, F.S. Cohen, P.S. Blank, and J. Zimmerberg. 2016. The hemifusion structure induced by Influenza virus haemagglutinin is determined by physical properties of the target membranes. Nat Microbiol. 1: 16050.

2. Gui, L., J.L. Ebner, A. Mileant, J.A. Williams, and K.K. Lee. 2016. Visualization and Sequencing of Membrane Remodeling Leading to Influenza Virus Fusion. J. Virol. 90: 6948–6962.

3. Chlanda, P., O. Schraidt, S. Kummer, J. Riches, H. Oberwinkler, S. Prinz, H.-G. Kräusslich, and J.A.G. Briggs. 2015. Structural Analysis of the Roles of Influenza A Virus Membrane-Associated Proteins in Assembly and Morphology. J Virol. 89: 8957–8966.

4. Kukulski, W., M. Schorb, S. Welsch, A. Picco, M. Kaksonen, and J.A.G. Briggs. 2012. Precise, correlated fluorescence microscopy and electron tomography of lowicryl sections using fluorescent fiducial markers. Methods Cell Biol. 111: 235–257.

5. Schorb, M., L. Gaechter, O. Avinoam, F. Sieckmann, M. Clarke, C. Bebeacua, Y.S. Bykov, A.F.-P. Sonnen, R. Lihl, and J.A.G. Briggs. 2017. New hardware and workflows for semi-automated correlative cryo-fluorescence and cryo-electron microscopy/tomography. J Struct Biol. 197: 83–93.

6. Schindelin, J., I. Arganda-Carreras, E. Frise, V. Kaynig, M. Longair, T. Pietzsch, S. Preibisch, C. Rueden, S. Saalfeld, B. Schmid, J.-Y. Tinevez, D.J. White, V. Hartenstein, K. Eliceiri, P. Tomancak, and A. Cardona. 2012. Fiji: an open-source platform for biological-image analysis. Nat. Methods. 9: 676–682.

7. Schneider, C.A., W.S. Rasband, and K.W. Eliceiri. 2012. NIH Image to ImageJ: 25 years of image analysis. Nat. Methods. 9: 671–675.